RSC Advances

PAPER

View Article Online
View Journal | View Issue

Cite this: *RSC Adv.*, 2023, **13**, 32185

Water-soluble fluorescent chemosensor for sorbitol based on a dicationic diboronic receptor. Crystal structure and spectroscopic studies†

Julio Zamora-Moreno, *[a] María K. Salomón-Flores, [a] Josue Valdes-García, [a] Cristian Pinzón-Vanegas, [a] Diego Martínez-Otero,[ab] Joaquín Barroso-Flores, [ab] Raúl Villamil-Ramos,[c] Miguel Á. Romero-Solano [a] and Alejandro Dorazco-González *[a]

Selective recognition of saccharides by phenylboronic dyes capable of functioning in aqueous conditions is a central topic of modern supramolecular chemistry that impacts analytical sciences and biological chemistry. Herein, a new dicationic diboronic acid structure **11** was synthesized, structurally described by single-crystal X-ray diffraction, and studied in-depth as fluorescent receptor for six saccharides in pure water at pH = 7.4. This dicationic receptor **11** has been designed particularly to respond to sorbitol and involves two convergent and strongly acidified phenyl boronic acids, with a pK_a of 6.6, that operate as binding sites. The addition of sorbitol in the micromolar concentration range to receptor **11** induces strong fluorescence change, but in the presence of fructose, mannitol, glucose, lactose and sucrose, only moderate optical changes are observed. This change in emission is attributed to a static complexation photoinduced electron transfer mechanism as evidenced by lifetime experiments and different spectroscopic tools. The diboronic receptor has a high affinity/selectivity to sorbitol (K = 31 800 M^{-1}) over other saccharides including common interfering species such as mannitol and fructose. The results based on ^{1}H, ^{11}B NMR spectroscopy, high-resolution mass spectrometry and density functional theory calculations, support that sorbitol is efficiently bound to **11** in a 1 : 1 mode involving a chelating diboronate–sorbitol complexation. Since the experimental B···B distance (5.3 Å) in **11** is very close to the calculated distance from the DFT-optimized complex with sorbitol, the efficient binding is attributed to strong acidification and preorganization of boronic acids. These results highlight the usefulness of a new diboronic acid receptor with a strong ability for fluorescent recognition of sorbitol in physiological conditions.

Received 12th September 2023
Accepted 24th October 2023

DOI: 10.1039/d3ra06198a

rsc.li/rsc-advances

Introduction

Selective recognition of polyols such as saccharides by synthetic boronic acids-based compounds remains a relevant area in supramolecular chemistry and analytical sciences due to applications in sensing,[1,2] separation,[3,4] glycoprotein manipulation,[5] bioimaging,[6] dynamic covalent assemblies,[7] clinical diagnostic of sugars-related diseases[8,9] medicinal chemistry,[10] and the understanding of new concepts in the molecular recognition field.[11]

In recent decades, the use of boronic acid derivatives has been proven to be an outstanding strategy for the recognition of saccharides,[12–17] glucosamine,[18] catecholamines,[19] nucleotides,[20] ginsenosides,[21] sialic acid,[22] glycated hemoglobin[23] and in general, 1,2-dihydroxy-substituted compounds.[24]

The affinity of phenylboronic acids towards 1,2-diol derivatives is primarily induced by the reversible formation of diol–boronic ester in an sp^2 hybridization, which results in increasing the Lewis acidity of the boron atom and subsequent fast conversion to the diol–boronate ester with an sp^3 hybridization.[25,26] In principle, the binding strength of boronic acid–diol ester depends on the orientation of the target analyte's hydroxyl groups,[27] the acidity of the boronic acid,[2] and the influence of substituent groups that can stabilize the sp^3-boronate ester.[25,28] The optimal pH for tetrahedral–boronate ester formation occurs ideally at a halfway pK_a value between the boronic acid and diol; however, it is well-known that this may vary depending on solvent, buffer composition, as well as the substituent groups in the boronic acid.[28,29]

[a]*Institute of Chemistry, National Autonomous University of Mexico, Ciudad Universitaria, México 04510, Mexico. E-mail: julio_zm@uaem.mx; adg@unam.mx*
[b]*Centro Conjunto de Investigación en Química Sustentable, UAEM-UNAM, Instituto de Química, Universidad Nacional Autónoma de México, C. P. 50200 Toluca, Estado de México, Mexico*
[c]*Centro de Investigaciones Químicas-IICBA, Universidad Autónoma del Estado de Morelos, Av. Universidad 1001 Col. Chamilpa, Cuernavaca, Morelos C.P. 62209, Mexico*

† Electronic supplementary information (ESI) available. CCDC 2281178. For ESI and crystallographic data in CIF or other electronic format see DOI: https://doi.org/10.1039/d3ra06198a

Simple phenylboronic acid (PBA, pK_a ~ 8.8) has too low binding constants for saccharides (<250 M^{-1}),[30] to achieve greater affinity, more sophisticated receptors are required. Thus, there is interest in creating water-soluble phenylboronic acid receptors with pK_a values less than physiological pH. However, this is an ongoing challenge, and it is not a trivial task.

Open-chain polyols, such as sorbitol and mannitol are biochemical metabolic intermediates and have been used as medicines. Sorbitol is among the food industry's most widely used sweetener substitutes for glucose and as thickener.[31,32] Some studies have shown that sorbitol is related to secondary effects in humans.[33] Among different sorbitol sensing methods, fluorescence is desired due to its known high sensitivity and rapid analytical signal.[34] While the need for highly selective and efficient chemosensors for sorbitol is evident, up until now, very few examples have been described compared to fructose and glucose.[35–37]

Optical recognition of sorbitol can be achieved by neutral diboronic acid dyes bearing aminomethyl groups (see Scheme 1) such as aminomethyl-naphthalene **1**,[38] aminomethyl-anthracene **2**,[39] binaphthalene-dimethanamine **3**,[40] carboxamide-quinoline **4-5**.[32,41] These fluorescent diboronic acids with amines typically show apparent binding constants between 350 and 10 000 M^{-1} where the sp^3-boronate ester is stabilized by the boron–nitrogen (amine) interaction. Consequently, they are suitable to sense at the micromolar concentration range, but not significantly lower. Many of these chemosensors require an organic cosolvent or basic conditions (pH > 8.0) to operate, which seriously hampers the intended applications. Furthermore, some still suffer some drawbacks such as too arduous synthesis and low selectivity to sorbitol.

To the best of our knowledge, the literature features only two examples of fluorescent chemosensors for selective recognition of sorbitol in pure buffered water based on monoboronic acids bearing naphthalimide **6**,[42] and benzo-thiophenes **7** (ref. 43) that operate with modest affinity, (K < 4000 M^{-1}). Overcoming these drawbacks should be feasible by using a hydrostable fluorescent diboronic receptor with pK_a values close to physiological pH.

A successful strategy for the acidification of boronic acids is the insertion of positive charges into the receptor scaffold as was evidenced by Geddes in several quinolinium dyes covalently attached to monoboronic acids where pK_a values dropped two units compared to the simple phenylboronic acid. These quinolinium-nucleus appended phenylboronic acids have been studied as optical sensors only for fructose, glucose and F^-.[44–46]

Recently, we demonstrated successful applications of a set of cationic receptors based on scaffolds of 2,6-pyridinedicarboxamide containing diboronic acids such as compound **8** for recognition of saccharides in an aqueous phase at physiological pH with a selectivity towards sorbitol and glucose.[47]

Previous studies have shown that bisquinolinium pyridine-2,6-dicarboxamide dyes from 6-aminoquinoline possess greater solubility in water and better photophysical properties compared to 3-aminoquinoline derivatives such as isomer **8**.[56]

Taking this into account, we surmised that an efficient sorbitol chemosensor could be achieved based on cationic diboronic acids attached to a fluorescent and semi-rigid scaffold able to orientate the boronic acids convergently.

In this study, we reported the results obtained for a water-soluble bisquinolinium pyridine-2,6-dicarboxamide salt bearing two strongly acidified boronic acids, including synthesis, crystal structure, acid–base properties, spectroscopic sensing studies of biological polyols and DFT calculations.

Results and discussion

Synthesis and structural analysis

For these investigations, the bromide salt of bisquinolinium diboronic acid **11** was successfully obtained by the procedure depicted in Scheme 2.

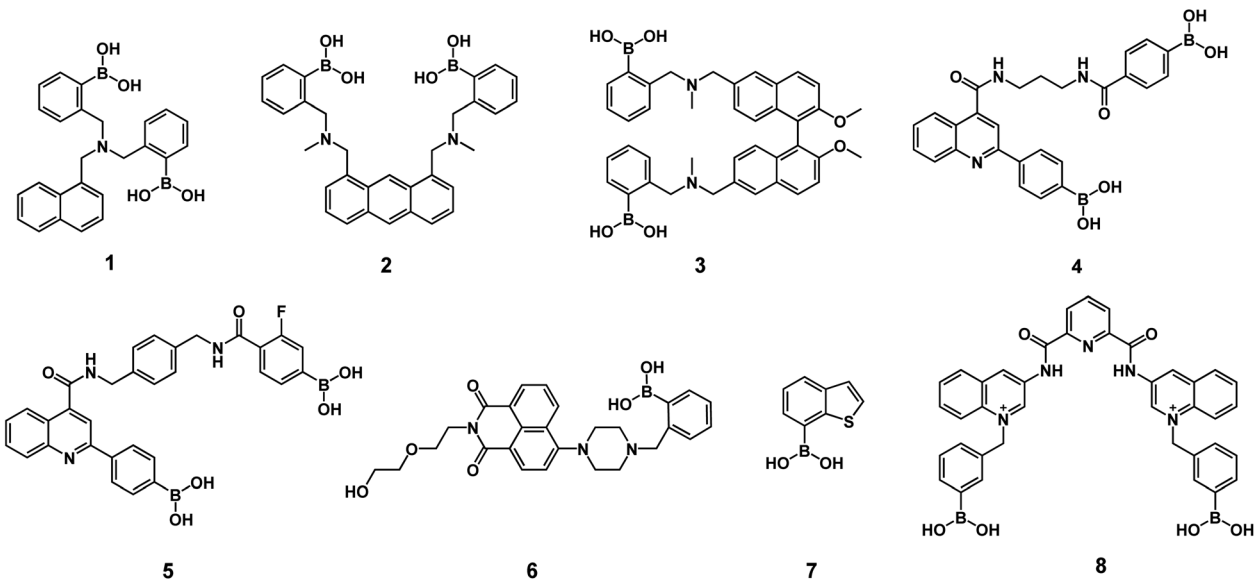

Scheme 1 Fluorescent phenylboronic acids-based chemosensors for D-sorbitol.

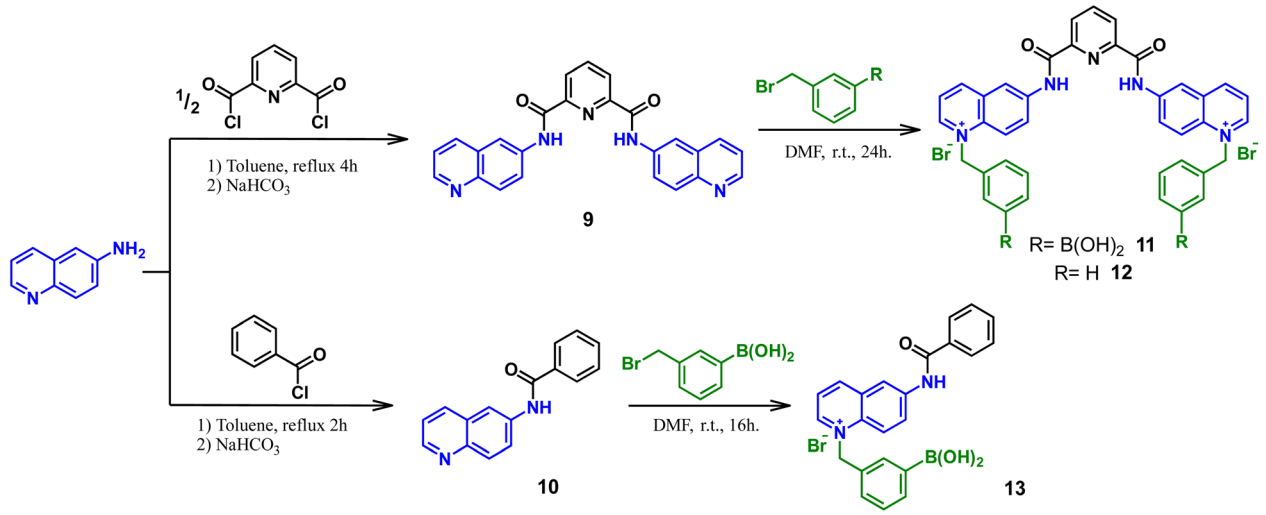

Scheme 2 General synthesis route of compounds **11–13** derived from 6-aminoquinoline.

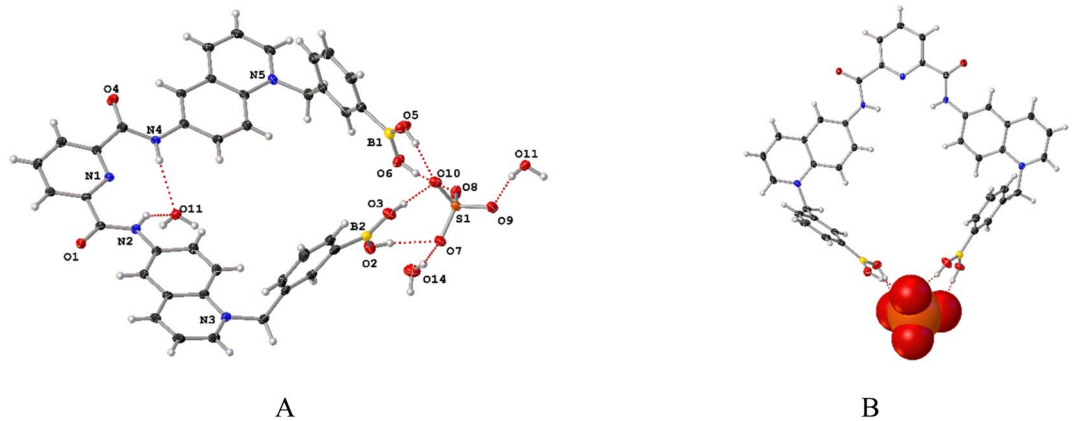

Fig. 1 (A) Perspective view of the X-ray structure of **11-SO$_4$** showing thermal ellipsoids drawn at 50% probability level. Hydrogen bonds B–O–H···O, N–H···O$_{water}$ and O–H···O–S are shown as red dashed lines. Occluded DMSO molecules were omitted for clarity. (B) Interaction between sulfate (space-filling model) and receptor **11** *via* hydrogen bonds B–O–H···O. Water and DMSO molecules were omitted for clarity.

A reference compound lacking boronic acid moiety **12** and a related quinolinium mono-boronic acid **13** were also prepared for comparative purposes. Two steps were involved in the formation of compounds **11–13**. First, the nucleophilic acyl substitutions were carried out by 6-aminoquinoline towards the appropriate acyl chloride in dry toluene under a N_2 atmosphere, to obtain compounds **9** and **10** which were confirmed by ^{1}H and ^{13}C NMR-spectroscopy (Fig. S1–S4†). Subsequently, *N*-alkylation products were obtained as bromide salts in good yields by the prolonged treatment with the corresponding (bromomethyl)-aryl reagent at r. t. in anhydrous DMF. The salts **11–13** were obtained as pale-yellow powders and pure according to ^{1}H, ^{13}C, ^{11}B NMR measurements, IR, high-resolution mass spectrometry and elemental analysis (C, H, N), see Fig. S5–S17.†

^{11}B NMR measurements of **11** and **13** were obtained in a CD_3-OD at 298 K. The spectra showed a broad signal centered at 27.4 ppm and 28.6 ppm for **11** and **13**, respectively, consistent with the sp^2-hybridized boron atom (Figs. S8 and S16†).[48] Efforts to obtain single crystals of the bromide salt of **11** suitable for X-ray diffraction analysis were not successful. Possibly due to electrostatic repulsion between dicationic organic units, which cannot be stabilized with small anions such as bromide.

However, X-ray single-crystal structure of **11** was obtained as a sulfate trihydrated salt by an anion metathesis with $NaSO_4$ from a mixture of H_2O–DMSO (v/v, 99/1) by slow evaporation (see Table S1 in the ESI for crystallographic data†). Geometric parameters for bond lengths, angles around B atoms, hydrogen bonds and π–π stacking interactions within the crystal packing of **11-SO$_4$** are compiled in Tables S2–S5.† Fig. 1A shows a perspective view of the molecular structure of **11-SO$_4$** and it confirms the presence of sp^2-hybridized boron atoms and trigonal geometries ($\Sigma\measuredangle_{(X-B1-X)}$ = 360.0° and $\Sigma\measuredangle_{(X-B2-X)}$ = 359.99°) which is consistent with its ^{11}B NMR spectrum. Both phenylboronic acids are directed at the same side of the molecule and they are separated by a B···B distance of 5.30 Å which is

Table 1 Absorption and emission maxima in buffered (10 mM, MOPS) pure aqueous solutions at pH = 7.4 and pK_a values of compounds **11–13**

		Spectrophotometric titration				Fluorimetric titration	
	λ_{abs} (log ε)	pK_{a1}-B(OH)$_2$	pK_{a2}	pK_{a3}	λ_{em}[a] (nm)	pK_{a1}(BOH$_2$)	pK_{a2}
11	274(4.47), 350(3.87)	6.62 ± 0.11	8.90 ± 0.05	11.34 ± 0.06	463	6.61 ± 0.07	8.18 ± 0.10
12	272(4.93), 355(4.00)	—	8.50 ± 0.07	11.34 ± 0.09	464	8.37 ± 0.07	10.62 ± 0.21
13	271(4.80), 325(4.01), 350(3.80)	8.05 ± 0.10	10.48 ± 0.08	—	473	7.74 ± 0.10	8.96 ± 0.05

[a] λ_{ex} = 350 nm for **11-12**; λ_{ex} = 325 nm for **13**.

structurally suitable for recognizing polyols in terms of the receptor preorganization.

In the reported structure of **8** that corresponds to an isomer of **11**, the B···B distance is approximately 2.0 Å longer than in the crystal of **11**. Importantly, all four –B–OH groups are oriented toward the sulfate anion, forming four hydrogen bonds B–OH···O as shown in Fig. 1B (Table S2†).

Clearly, the sulfate anion induces the convergence of the boronic acid groups. Thus, receptor **11** possibly could function as a receptor for oxoanions *via* cooperative hydrogen bonds.

The crystal of **11-SO$_4$** is strongly hydrated; two $(H_2O)_3$ clusters are confined in the unit cell (Fig. S18†) with the consequence that the receptor cavity is occupied by a water molecule where the N–H bonds of both amide groups form two N–H···O hydrogen bonds. This high degree of hydration is evidence of its hydrostability in the solid state. The receptor **11-SO$_4$** possesses a high degree of planarity between quinolinium rings and the central pyridine ring with dihedral angles between 5.54° and 8.48°. The two amide groups are directed inside the receptor cleft. This *syn–syn* conformation of amide groups has been usually described for crystals of pyridine-2,6-dicarboxamide pincer-like derivatives as a consequence of intramolecular H bonds of type N–H···N$_{pyridine}$.[49–53]

An inspection of the crystal of **11-SO$_4$** displays multiple π–π interactions mainly centered on the quinolinium rings and the central pyridine involving cofacial parallel stacked geometries with centroid–centroid distances ranging from 3.49 Å and 3.80 Å (Fig. S19 and Table S5†). These strong interactions can be ascribed to the positive electrostatic potential around the quinolinium rings.

Optical and acid–base properties

The bromide salts of cationic compounds **11–13** are soluble in buffered (10 mM MOPS pH = 7.4) pure water and follow very well the Lambert–Beer law up to 100 μM; thus, these conditions and a concentration within this range were used for further spectroscopic studies.

The absorption and emission properties of bromide salts of compounds **11–13** are compiled in Table 1 and the family of UV-vis/fluorescence spectra at different pH values for **11** and **12** are displayed in Fig. 2A–D. In general, the salts **11–13** have strong absorption maxima at $\lambda \sim 271-274$ nm with lower-energy absorption shoulders at $\lambda \sim 325-350$ nm attributed to intraligand $\pi \rightarrow \pi^*$ electronic transitions centered in the *N*-alkyl quinolinium fragment.[54] The blue emission in these quinolinium-based compounds is typically attributed to intramolecular charge transfers (ICTs) in the excited state.[55] Compound **11** possesses four ionogenic groups: two equivalent PBA moieties and two amide groups.

The reference compound **12,** lacking PBA moieties, has only two amide groups and monoboronic compound **13** contains one PBA moiety and one amide group. The positive charges on the quinolinium rings must acidify these groups. Thus, acid–base properties of bromide salts of **11–13** were explored by fluorescence and UV–Vis pH titrations.

For bromide salt of **12**, two pK_a values were estimated, pK_{a1} = 8.50 and pK_{a2} = 11.34, from UV-vis pH titration and two values were calculated from fluorescence *versus* pH titration, pK_{a1} = 8.37 and pK_{a2} = 10.62 (see insets Fig. 2C and D). These pK_a values are similar to those we reported for the triflate salt of **12** and unambiguously assigned to amide groups.[53] Total deprotonation of amide groups in **12** induced a strong decrease in emission intensity, practically generating a non-emitting species, probably by an intramolecular photoinduced electron transfer (PET).

Results of UV-vis pH titration for **11** are shown in Fig. 2A. The formal fit of the absorbance (325 nm) *versus* pH curve to the theoretical equation allows us to estimate clearly three pK_a values (pK_{a1} = 6.62, pK_{a2} = 8.90 and pK_{a3} = 11.34, Table 1). The two values above 8.50 can be attributed to the two amide groups compared to compound **12**. The diboronic isomer **8** that we have recently reported, has pK_a values less than 7.0 assigned to the boronic groups.[47]

The fluorimetric titration experiment shows that emission quenching of **11** is mainly controlled by the dissociation of a group with a pK_a below 7.0 (Fig. 2B). The emission data at 463 nm can be very well fitted to two pK_a values (see inset, Fig. 2B), pK_{a1} = 6.61 and pK_{a2} = 8.18.

The absence of a third pK_a value in the fluorescence curve can be explained by the formation of a non-emitting conjugated base, after deprotonation of boronic acid and an amide group. In our experience, completely deprotonated (pH > 10) quinolinium pyridine-2,6-dicarboxamide derivatives are practically not fluorescent.[47,49,56] The first pK_{a1} = 6.61 of **11** is comparable to those reported values for structurally related monoboronic acids appended quinolinium rings studied by Geddes which have pK_a less than 7.0 assigned to the boronic groups from fluorescence data.[44–46]

To unambiguously assign the pK_a value of boronic acid in **11**, we reproduced the UV-vis pH titration in the presence of

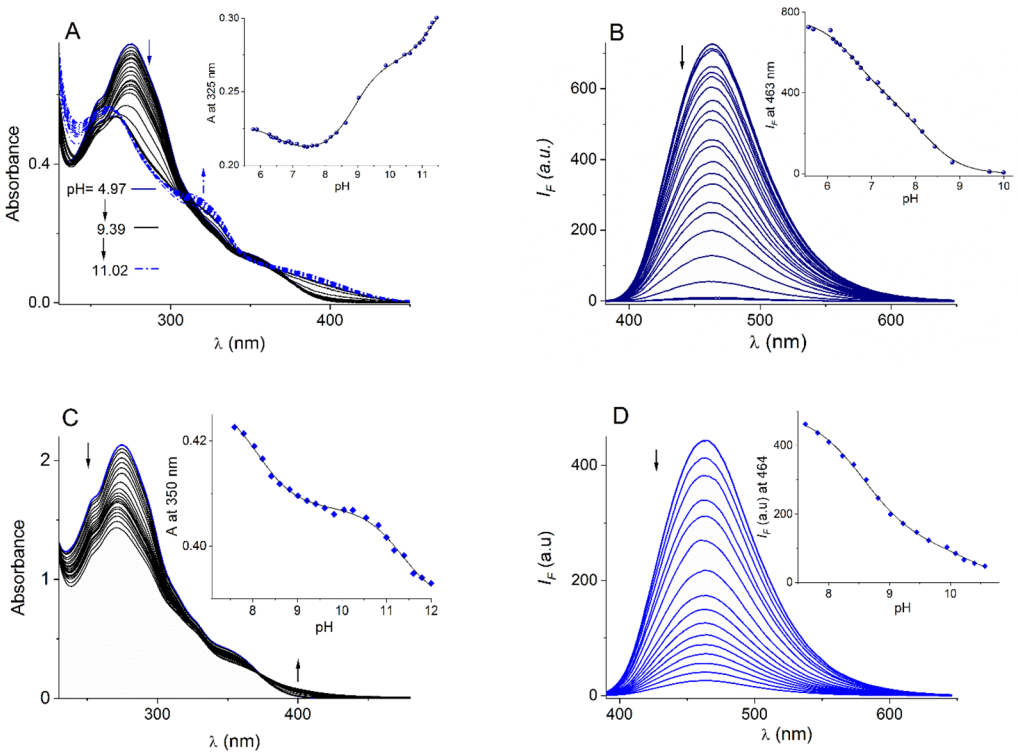

Fig. 2 UV-vis pH-titration (A) and fluorescence pH-titration (B) of buffered aqueous solutions of the bromide salt of **11** (25 μM). UV-vis pH-titration (C) and fluorescence pH-titration (D) of buffered aqueous solutions of the bromide salt of **12** (25 μM). The insets show pH-titration curves observed at absorbance and emission maxima for both receptors at 25 °C and the solid lines were obtained by fitting the experimental data to the corresponding theoretical equation for three or two pK_a values.

fructose (10 mM), see Fig. S20,† with the baseline expectation of having a considerable drop in the pK_a value only for the corresponding boronic acid.[44] Fig. 3 shows UV-vis pH profiles of **11** (25 μM) in the absence and presence of this sugar. The absorbance at 325 nm *versus* pH in the presence of fructose can be well fitted to three pK_a values (pK_{a1} = 5.58, pK_{a2} = 8.71 and pK_{a3} = 11.30). Adding fructose induces a strong drop in the first pK_a of 1.12 units compared to the estimated value without fructose (*vide supra* Table 1). In contrast, the two pK_a values above 8.5 remain practically constant as is shown in inset Fig. 3, suggesting that these correspond to the two amide groups. This finding is significant because it evidences that boronic acid groups of **11** are converted in their anionic tetrahedral sugar binding forms at pH values close to the physiological value of 7.4 without interference from the ionization of the amide groups.

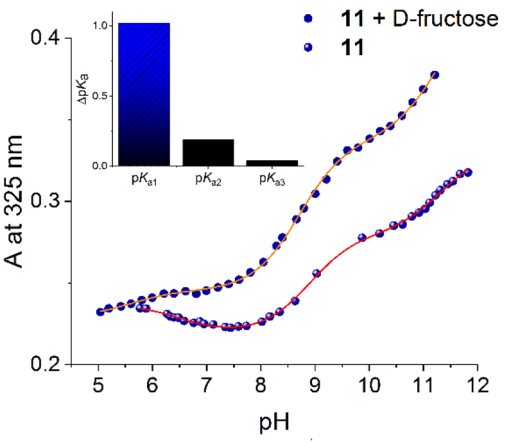

Fig. 3 UV-vis pH titration profiles at 325 nm of buffered aqueous solutions **11** (25 μM) in the absence and the presence of fructose (10 mM). Solid lines were obtained by fitting the experimental data to the theoretical equation for three pK_a values.

Fluorescent saccharide recognition

To test the affinity of **11** towards saccharides, a series of fluorescence titration experiments were performed with two open-chain polyols (sorbitol and mannitol), and "small" saccharides (fructose, galactose, glucose, myo-inositol, lactose and sucrose) at pH = 7.4. In general, adding these polyols to buffered aqueous solutions of **11** shows reproducible quenching effects with a selective peak for sorbitol.

Fluorimetric titration of **11** (20 μM) with sorbitol is shown in Fig. 4A, the fluorescence intensity drops 4 times at saturation (~0.4 mM) and the titration profile at 463 nm perfectly fits a 1 : 1 binding mode by a nonlinear least-squares treatment using eqn (1) to give apparent binding constant of $K_{(\mathbf{11}\text{-sorbitol})}$= (3.18 ± 0.10) × 10^4 M^{-1}, where I_F is the observed intensity, I_0 is the intensity of the free receptor, ΔI_∞ is the maximum intensity change induced by the presence of the saccharide at saturation,

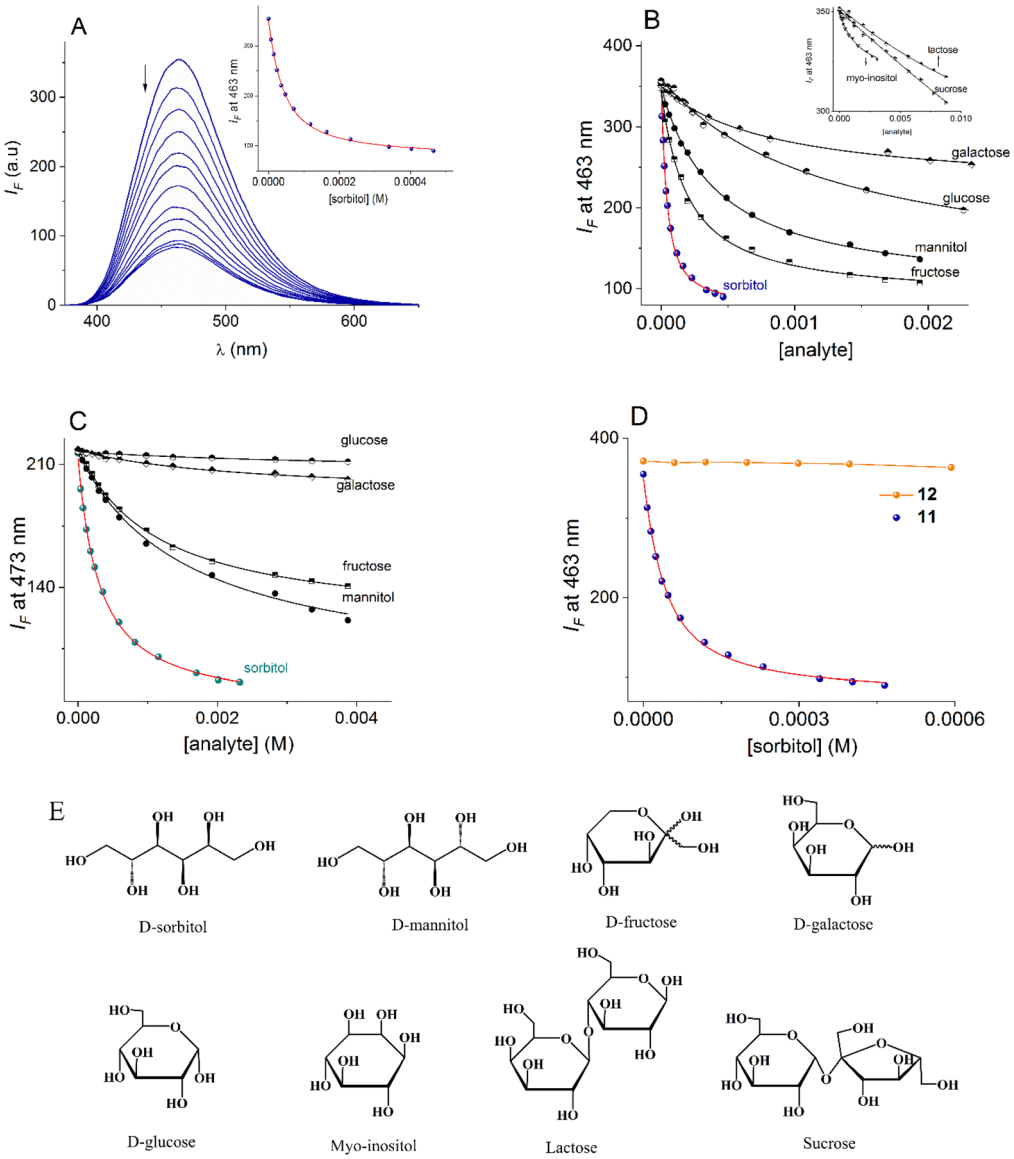

Fig. 4 (A) Changes in the emission spectra (λ_{ex} = 350 nm) of buffered aqueous solution **11** (20 μM) upon the addition of increasing amounts of sorbitol (0–480 μM) at pH = 7.40. Fluorimetric titration profiles of aqueous solutions of (B) **11** and (C) **13** (20 μM in both cases) upon the addition of increasing amounts of polyols and monosaccharides at pH = 7.4. The solid lines were obtained by fitting to eqn (1). (D) Fluorimetric titrations of **11** and **12** with sorbitol. (E) Polyols used in this work.

$[G]_T$ is the total concentration of the saccharide, and K is the apparent binding constant.[57]

$$I_F = I_H + \frac{\Delta I_\infty \left\{ [H]_T + [G]_T + \frac{1}{K} - \left[\left([H]_T + [G]_T + \frac{1}{K} \right)^2 - [4][H]_T[G]_T \right]^{0.5} \right\}}{2[H]_T} \quad (1)$$

The apparent binding constants of **11** with the rest of the saccharides were estimated under the same conditions. The corresponding fluorimetric titration profiles are shown in Fig. 4B and their respective affinities are compiled in Table 2. For comparison, the data includes the apparent stability constants of PBA with saccharides at pH = 7.4, taken from the literature.[30]

All systems showed the formation of a 1 : 1 model with good quality fits (error < 10%). Noteworthy that the chemical equilibrium boronic acid–boronate ester was reached within 1.0 min after the addition of the polyol aliquot. This relatively fast equilibrium is not so common[58] and probably due to the strong acidification of boronic acids. The structure of all saccharides screened is shown in Fig. 4E.

Overall, sucrose, lactose, myo-inositol, glucose and galactose gave a very low quenching effect (I_F/I_0 < 1.4) upon the addition of 1.0 mM of polyol and low affinities were estimated. The

Table 2 Apparent binding constants K (M^{-1}) for bromide salts of **11** and **13** (20 μM) with monosaccharides and polyols in water at pH 7.4

	11		**13**		PBA
Analyte	$K_{(1:1)}$	I_F/I_0 [a]	$K_{(1:1)}$ [b]	I_F/I_0 [a]	K [c]
D-sorbitol	$(31.83 \pm 0.11) \times 10^3$	4.21	$(2.20 \pm 0.08) \times 10^3$	2.16	370
D-fructose	$(4.37 \pm 0.05) \times 10^3$	2.73	$(1.09 \pm 0.06) \times 10^3$	1.33	160
D-mannitol	$(2.96 \pm 0.12) \times 10^3$	2.10	$(0.92 \pm 0.05) \times 10^3$	1.37	120
D-galactose	$(0.99 \pm 0.09) \times 10^3$	1.26	$(0.40 \pm 0.04) \times 10^3$	1.05	15
D-glucose	$(0.68 \pm 0.04) \times 10^3$	1.40	$(0.20 \pm 0.02) \times 10^3$	1.03	4.6
Myo-inositol	$(0.43 \pm 0.07) \times 10^3$	1.05	[b]	1.01	—
Lactose	$(0.17 \pm 0.03) \times 10^3$	1.03	[b]	1.01	1.6
Sucrose	$(0.07 \pm 0.01) \times 10^3$	1.04	[b]	1.02	0.6

[a] I_F/I_0 indicates the quenching relative selectivity parameter at 463 nm for **11** and 474 nm for **13** in the presence of 1.0 mM of the polyol or monosaccharide. [b] Undetected association. [c] Binding constants reported in an aqueous medium at pH = 7.4, ref. 30.

addition of mannitol and fructose resulted in a considerable quenching effect ($I_F/I_0 \sim 2.5$), but it was still significantly lower than that observed for sorbitol. In general, the affinity of **11** towards studied saccharides is one or two orders of magnitude lower than that estimated for sorbitol including fructose, making this chemosensor ideal for achieving selective detection of sorbitol at physiological pH.

Next, the affinity of related quinolinium mono-boronic acid **13** was evaluated with the saccharides by fluorescence; the titration profiles are shown in Fig. 4C. The affinity trend is parallel to that reported for PBA with common monosaccharides; fructose > galactose > glucose (see Table 2), which is not unexpected because it is well-known that simple monoboronic acids possess inherent selectivity to fructose.[59] Regarding to sorbitol, the affinity of the monoboronic compound **13** is one order of magnitude less than that calculated for diboronic **11**. These data suggest that compound **11** may involve a cooperative chelating diboronate binding sorbitol.

On the other hand, fluorescent sensing of monosaccharides by hydrophobic receptors lacking boronic acids as a result of a disaggregation mechanism has recently been reported.[58] To discard this mechanism and incidentally verify the participation of the boronic acids of compound **11** in the molecular recognition, we test the effect of sorbitol on the fluorescence of reference compound **12** in the same concentration range and the same pH as that for diboronic receptor **11**, and practically no effect was observed as shown in Fig. 4D.

Since compound **11** has two boronic acid-based binding points, the 1 : 1 binding mode observed by fluorescence experiments can be rationalized as (1) chelation of the saccharides by both boronic acid groups or (2) simultaneous binding to each boronic acid group operating independently with a similar quenching effect and apparent binding constants, in this option, the estimated K values must be multiplied by a factor of 2.

The first possibility is feasible, considering that compound **11** is symmetrical, semi-rigid and has both boronic acid groups oriented in the same position according to its crystalline structure. The relatively short B···B distance of 5.30 Å could be further shortened for the presence of flexible methylene linkers.

Fig. 5 shows the correlation between Log K_{PBA} and Log K values for compounds **11** and **13** at pH = 7.4. For diboronic **11**, there is observed a lineal correlation for saccharides, except for sorbitol which shows a strong positive deviation. Glucose also shows this positive bias but to a lesser extent. In contrast, for monoboronic **13**, all saccharides, including sorbitol, have a good linear correlation which is expected for diol complexation involving only one boronic acid.

A plausible interpretation of the high affinity of **11** for sorbitol is that this diboronic compound effectively binds as a ditopic chelate. To further insight into the quenching response, the lifetimes of **11** in the absence and presence of sorbitol were measured. An aqueous solution of **11** upon excitation with a 354 nm laser exhibited a bi-exponential decay with lifetimes $\tau_1 = 5.18$ and $\tau_2 = 2.00$ ns (Fig. 6). The lifetime of solution of **11** after the addition of a concentrated solution of sorbitol (12 equiv.) has a negligible change of lifetime values and form of decay profile, indicating that static quenching is dominant in the quenching mechanism.[60] Furthermore, similar lifetime values and the same shape of the spectra without shift of maxima in the fluorimetric titration of **11** with sorbitol (Fig. 2A) suggest that the transition energy is virtually the same in the two compounds and that the emission comes from the singlet state of quinolinium groups.

Interaction studies by NMR and high-resolution mass spectrometry

To support the formation of ester boronate of **11** with sorbitol, we performed ^{1}H and ^{11}B NMR spectroscopic measurements. Fig. 7A illustrates a titration experiment of **11** (2.0 mM) with sorbitol monitored by ^{1}H NMR in DMSO-d_6. Upon increasing the concentration of sorbitol (0–4.0 equiv.), only the aromatic protons (H_{ptsr}) from phenyl boronic moieties (see Fig. 7A for the proton label) are clearly affected. This set of aromatic protons shows a considerable upfield shift of about 0.40 ppm along with the simultaneous disappearance of the protons of –$B(OH)_2$ at 8.19 ppm (red box).

In principle, this shift can be attributed to reversible boronate esterification with diol fragments from the sorbitol due to the appearance of the negative charge on the boron atom. The

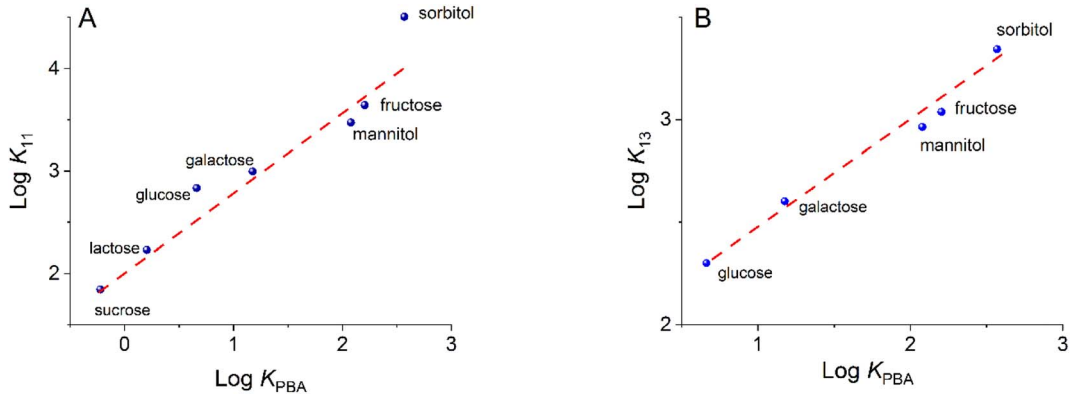

Fig. 5 Log of apparent binding constants for **11** (A) and **13** (B) *versus* Log of binding constants for PBA at a pH of 7.4. Red dashed lines correspond to the slope unity.

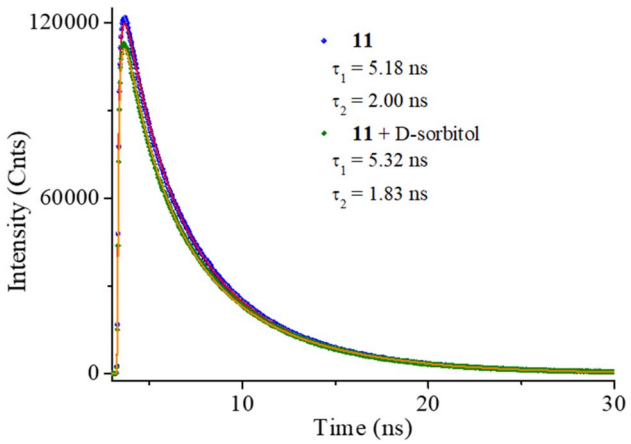

Fig. 6 Emission decay profiles of aqueous solutions of **11** in the absence and presence of 12 equiv. of sorbitol at pH = 7.4.

signals of the rest of the protons of **11** are practically unaffected. The sorbitol signals (orange box, Fig. 7A) in the titration broaden over time, possibly due to deuterium exchange with the solvent.

The change of hybridization of the B atoms in **11** from neutral trigonal-sp^2 boronic acid to anionic tetrahedral-sp^3 boronate generated by esterification with sorbitol was observed by ^{11}B NMR experiments in CD_3OD-D_2O (Fig. 7B).

Upon the addition of 12 equiv. of sorbitol to a solution of **11** (5 mM) the initial signal for sp^2-B atom at 26.1 ppm disappeared and a new broadened signal at 10.2 ppm arose for sp^3-B atom. At r.t. (298 K), it was difficult to see the broadened signal of sp^3-B atom; however, at a low temperature of 233 K the signal can be clearly observed as is shown in Fig. 7B (bottom). This change in the chemical shift ($\Delta\delta$ = 16 ppm) of the ^{11}B NMR signals is characteristic of the formation of boronate complex with diols.[48,61]

Electrospray ionization (ESI) mass spectrometry has been used to study boronic acid–diol complexation.[47] Next, high-resolution electrospray mass experiments were carried out in the positive mode with solutions of compound **11** in the absence and presence of sorbitol in aqueous methanol. Fig. 8A shows the ESI-MS spectrum of free compound **11**, one charged state at m/z = 770.17943, for the monocationic $[R + Br]^+$ (R = the dicationic receptor **11**) is clearly observed and isotopically resolved. The signals separated by 1.0 unit match perfectly the theoretical isotopic distribution.

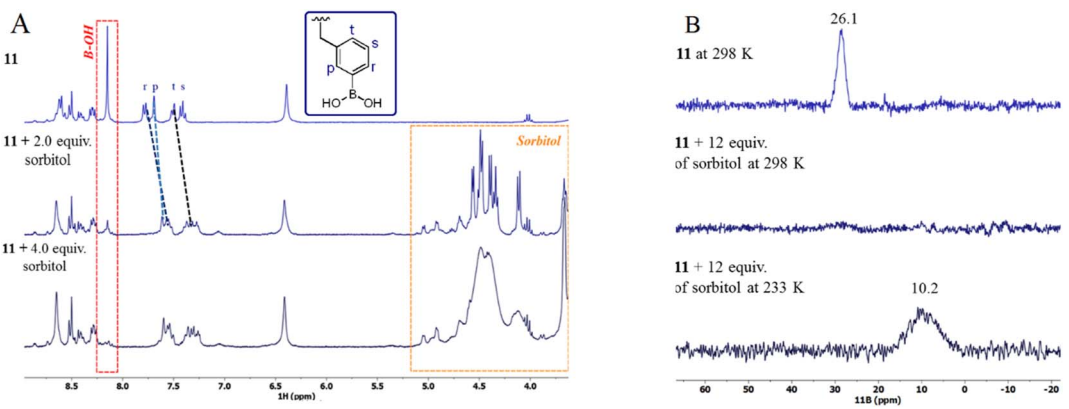

Fig. 7 (A) Partial ^{1}H NMR spectra (300 MHz, 298 K) of **11** (2.0 mM) in the absence and presence of increasing amounts of sorbitol (0, 2.0 and 4.0 equiv.). (B) ^{11}B NMR spectra (160.5 MHz) of **11** (5 mM) in the absence and presence of 12 equiv. of sorbitol in CD_3OD-D_2O at different temperatures (298 and 233 K).

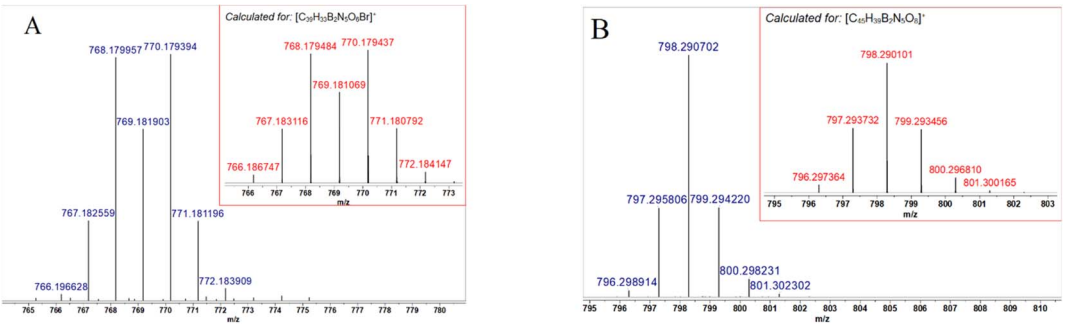

Fig. 8 ESI-HRMS spectra obtained by the positive scan of free bromide salt of **11** (A) and **11** in the presence of sorbitol (B) in neutral aqueous methanol. Insets: theoretical isotopic patterns.

Table 3 Theoretical and observed *m/z* values for ESI-HRMS peaks for **11** in the presence of sorbitol (R is the dication receptor **11**, $C_{39}H_{33}B_2N_5O_6^{2+}$)

	Species	Formula	Theoretical	Observed
14	$[R(sorbitol)(H_2O)_{4-} + H]^+$	$C_{45}H_{38}B_2N_5O_8^+$	798.29010	798.290702
15	$[R(sorbitol)(H_2O)_{4-} + Br]^+$	$C_{45}H_{39}B_2N_5O_8Br^+$	878.21626	878.217742
16	$[R(sorbitol)(H_2O)_{4-}(OH)_2 + K]^+$	$C_{45}H_{40}B_2N_5O_{10}K^+$	912.28584	912.285400

Fig. S21† shows the whole ESI-MS spectrum of the mixture **11** with sorbitol; the base peak at $m/z = 798.2907$ corresponds to one charged species for 1 : 1 complex with formula $[R(sorbitol)(H_2O)_{4-} + H]^+$ by exact mass and perfect coincidence with the theoretical isotopic distribution (see Fig. 8B and Table 3 entry 1). This signal has the multiplicity expected for a species containing two sp^3 boronate groups and one sorbitol molecule with the elimination of four water molecules evidencing the formation of four ester bonds. Eliminating four water molecules is only possible if both groups of boronic acid participate. This species contains two boronate groups that balance the positive charges of the quinolinium rings, therefore, it is neutral and undetectable by MS. However, it can easily be cationized by trapping H^+. Since the most abundant species detected by HRMS only contain one sorbitol molecule, the only possibility is the formation of a sorbitol chelate complex, which should has the chemical structure **14**.

Two less abundant one-charged species are also seen at $m/z = 878.2177$ and $m/z = 912.2854$ (see Table 3, entries 2-3). The first species matches $[R(sorbitol)(H_2O)_{4-} + Br]^+$ involving one sorbitol bound two trigonal sp^2 boronic groups through four ester bonds, the one charge and mass are consistent for the presence of a Br^- anion; this complex should have structure **15**.

The species at $m/z = 912.2854$ corresponds to $[R(sorbitol)(H_2O)_{4-}(OH)_2 + K]^+$ with one sorbitol bound two anionic hydroxo sp^3-boronate complexes, which are formed by the addition of a hydroxyl anion and four ester bounds as is shown in **16**.

All the species detected by masses correspond to a 1 : 1 complex with a chelate binding mode, which could explain the tight affinity to sorbitol (Scheme 3).

The assignments of signals of all species observed containing the dicationic compound **11**-sorbitol complex along with their exact experimental/calculated masses are shown in Table 3.

Considering the results of pH titration and the most intense peak from HRMS the species **14** involving chelated sp^3-boronate esters seems more plausible.

DFT calculations

To gain further insights into the recognition mode of **11** toward sorbitol, DFT calculations were performed for the species **14**. The geometry was optimized at the ωB97X-D/LANL2DZ level of theory with water as an implicit solvent under the SMD continuum solvation model. The complex showed positive vibrational frequencies which indicates the presence of a minimum on the potential energy surface, and therefore it represents a physically accessible conformation. Sorbitol coordinates three –OH groups for each boronic acid as is shown in Fig. 9.

It is noteworthy that the calculated B···B distance for the optimized macrocycle resulted from the 1 : 1 complex is 5.53 Å which is very close to 5.30 Å experimental value.

Discussion affinity towards sorbitol by recent boronic acids-based receptors

Table 4 collects apparent binding constants of sorbitol complexes for recent mono and diboronic receptors. An analysis of these binding data shows that receptor **11** has an affinity one to two orders of magnitude higher than that reported for PBA (Table 2 and Fig. 5), as well as monoboronic acid receptors **1**, **6** and **7** in water at pH = 7.4. This tight affinity can be assigned to the stronger Lewis acidity of dicationic **11** involving a pK_a value ~6.6 compared to $pK_a = 8.8$ of PBA or $pK_a > 7.0$ of **6-7**.

The neutral diboronic acid receptors **1**, **2** and **4** based on amine dyes possess considerably lower affinities than receptor

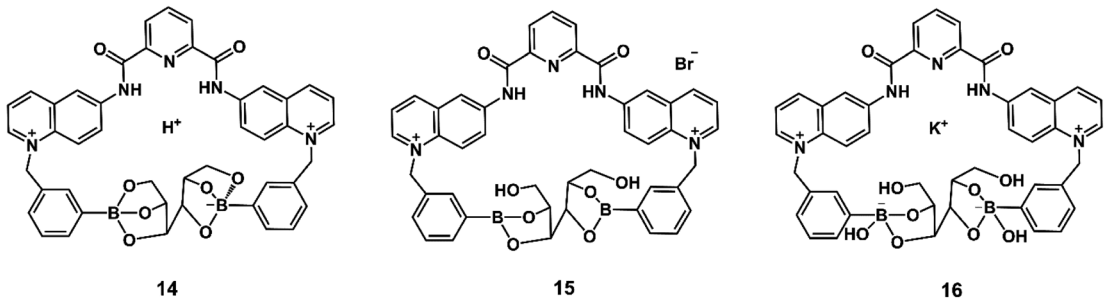

Scheme 3 Proposed structures of chelate sorbitol complexes **14–16** detected by HRMS.

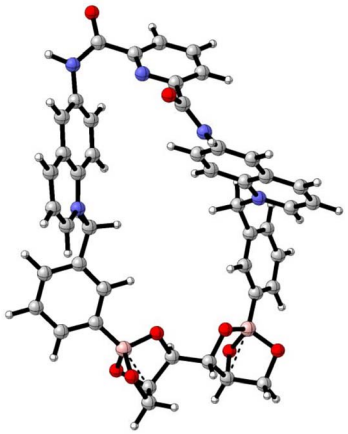

Fig. 9 DFT optimized structure at the ωB97XD/LANL2DZ level of theory for compound **14**.

Table 4 Apparent binding constants (M^{-1}) of sorbitol complexes with mono- and diboronic receptors in aqueous media at different pH values

Receptor	K (M^{-1})	Media	Ref.
1	340	pH = 8.0; H_2O/MeOH	38
2	1060	pH = 7.4; H_2O/MeOH	39
3	11 300	pH = 8.0; H_2O/MeOH	40
4	570	pH = 7.4; H_2O/DMSO	41
5	10 900	pH = 9.0; H_2O/DMSO	32
6	140	pH = 7.4; H_2O	42
7	4560	pH = 7.4; H_2O	43
8	6800	pH = 7.4; H_2O/MeOH	47
11	31 800	pH = 7.4, H_2O	This work

11, despite being studied in less competitive media such as aqueous mixtures with organic co-solvents. Neutral diboronic receptors **3** and **5** based on amine and quinoline, respectively, show close behavior to **11** but in basic conditions and in aqueous organic mixtures. The isomer **8**, recently reported by us, has an affinity three times lower than **12** despite having similar values to pK_a.

This effect probably reflects a cooperative chelating complexation with the participation of both boronic acids in **11**; it is not unexpected because the distance B···B in **11** is less (~2 Å) than that observed in the crystal of isomer **8**. The dicationic nature and acidity of the boronic acids in **11** make this compound useful for optical recognition of sorbitol at physiological pH.

The reduction of the pK_a value of phenylboronic acids is critical to achieving higher performance of receptor **11** in aqueous phase; however, other structural features are also significant such as the inclusion of two-point recognition, the preorganization of binding sites, and rigidity of bisquinolinium pyridine-2,6-dicarboxamide scaffold.[62]

Conclusions

We have introduced a new fluorescent cationic diboronic acid-based receptor **11** for the optical recognition of sugars with hydrostability, photostability, and strong ability for sorbitol optical sensing in micromolar concentration range in pure water at physiological pH. Under these conditions, the addition of sorbitol exhibits an efficient and fast quenching response of **11** with pronounced affinity (K = 31 800 M^{-1}) and selectivity over other common saccharides such as fructose, mannitol, glucose, lactose and sucrose. In terms of reactivity and chemical structure, diboronic receptor **11** possesses two strongly acidified boronic groups, with pK_a = 6.6, oriented towards the same plane with a proximity B···B of 5.3 Å as evidenced by its X-ray crystal structure. Lifetime measurements and fluorescence spectroscopy display that the quenching process could be explained as a static complexation PET mechanism. ^{1}H, ^{11}B NMR spectroscopy, HRMS measurements and DFT calculations show that sorbitol is efficiently bound to **11** in a 1 : 1 model involving a chelating sp^3 boronate–diol complexation.

The Log of the apparent binding constants for **11** with the studied saccharides correlates linearly with the Log of binding constants with simple phenylboronic acid; except for sorbitol which shows a strong positive deviation due to the chelating binding mode.

Among all the boronic acid receptors reported for sorbitol in aqueous media, diboronic **11** has the highest affinity.

Overall, these results further highlight the use of a new chemical approach of water-soluble diboronic acid receptors based on a cationic bisquinolinium pyridine-2,6-dicarboxamide scaffold with analytical applications for the fluorescent sensing of saccharides in aqueous media.

Experimental section

Bromide salts of **11–13** were prepared according to modified procedures reported previously.[47,53] The detailed procedure of intermediaries **9-10** and bromide salt of **12**, previously reported by us, is described in the ESI.†

Synthesis of 3,3′-((pyridine-2,6-dicarbonyl)bis(azanediyl)) bis(1-(3-boronobenzyl)quinolin-1-ium) dibromide, 11

The compound **9** (100.0 mg, 0.24 mmol) was dissolved in 5 mL of anhydrous DMF. Then, 2.2 equiv. of 3-(bromomethyl)-phenylboronic acid (90% purity, 125.2 mg, 0.52 mmol) were added and stirred for 24 h at r. t. under an N_2 atmosphere. A yellow sticky precipitate was obtained, and 1.0 mL of anhydrous DMF was added. The mixture was slurred for 2 h. Subsequently, 12.0 mL of ethyl acetate was added and stirred vigorously for 30 min, then cooled in an ice bath. The pale-yellow solid was isolated by vacuum filtration and washed with a 5.0 mL portion of a DMF/ethyl acetate mixture (1 : 4), and with 10 mL of diethyl ether. The solid was placed in a flask and **11** was extracted with 40 mL of deionized water. The volatiles were removed in a rotary evaporator at NMT 50 °C and the almost white solid was dried under reduced pressure to obtain the bromide salt of **11** (73%, 147.8 mg). Single crystals for X-ray diffraction analysis were obtained as sulfate salt by slow evaporation from a mixture of H_2O–DMSO (v/v, 99/1).

^{1}H NMR (300 MHz, 298 K, DMSO-d_6); δ 11.61 (s, 2H, $NH_{(amide)}$), 9.62 (d, $^3J_{HH}$ = 5.7 Hz, 2H, H_j), 9.22 ($^3J_{HH}$ = 8.7 Hz, 2H, H_h), 8.61–8.50 (m, 6H, $H_{i,\ m,\ l}$) 8.41 (m, 1H, H_a) 8.30 (pseudo-t, $^3J_{HH}$ = 6.9 Hz, 2H, H_b), 8.19 (broad-s, 4H, BOH), 7.78 (d, $^3J_{HH}$ = 7.2 Hz, 2H, H_r), 7.68 (s, 2H, H_p), 7.48 (d, $^3J_{HH}$ = 7.5 Hz, 2H, H_t), 7.40 (t, $^3J_{HH}$ = 7.5 Hz, 2H, H_s), 6.37 (s, 4H, CH_2). ^{13}C{^{1}H} NMR (100 MHz, 298 K, DMSO-d_6); δ 163.1 (carbonyl-C_d), 149.2 (C_j), 148.5 (C_c), 148.0 (C_h), 142.0 (C_a), 139.4 (C_e), 135.6 (C_q), 135.3 (C_k), 135.0 (C_r), 133.5 (C_o), 132.9 (C_p), 131.7 (C_g), 130.6 (C_i), 129.6 (C_t), 128.9 (C_s), 126.6 (C_m), 123.4 (C_b), 120.8 (C_l), 118.5 (C_f), 60.7 (methylene-C_n); ^{11}B NMR (160.5 MHz, 298 K, CD_3OD) δ 27.4 (broad signal); HRMS-ESI$^+$ (*m*/*z*): calculated for $[C_{39}H_{33}B_2N_5O_6Br]^+$: 768.179484, found: 768.179957. ATR-IR (cm^{-1}): 3218br, 1546s, 1378s, 1333s, 771m and 714m. Anal calcd. for $C_{39}H_{33}B_2Br_2N_5O_6$: C, 55.16; H, 3.92; N, 8.25. Found: C, 55.11; H, 3.98; N, 8.20.

Synthesis of 6-benzamido-1-(3-boronobenzyl)quinolin-1-ium bromide, 13

Compound **10** (100.0 mg, 0.40 mmol) was dissolved in 4.0 mL of anhydrous DMF. Then, 1.1 equiv. of 3-(bromomethyl)-phenylboronic acid (90% purity, 105.8 mg, 0.44 mmol) were added and stirred for 16 h. at r. t. under an N_2 atmosphere. The reaction turned yellow instantly, and that color was retained throughout the reaction time. The volume of the yellow solution was halved under vacuum at 40 °C in a rotary evaporator. Subsequently, 10 mL of cold ethyl acetate was added, forming a slurring precipitate at low temperature (ice bath) for 2 h. This precipitate was isolated by vacuum filtration and washed twice with cold ethyl acetate and diethyl ether at r. t. The yellow solid was dried under reduced pressure to obtain the bromide salt of **13** (91% mg). Anal calcd. for $C_{23}H_{20}BBrN_2O_3$: C, 56.65; H, 4.35; N, 6.05. Found: C, 56.47; H, 4.48; N, 6.0.

^{1}H NMR (400 MHz, 298 K, D_2O/CD_3CN); δ 9.17 (dd, $^3J_{HH}$ = 6.0 Hz, $^4J_{HH}$ = 1.6 Hz, 1H), 9.97 (d, $^3J_{HH}$ = 8.4 Hz, 1H), 8.59 (d, $^3J_{HH}$ = 2.4 Hz, 1H), 8.23 (d, $^3J_{HH}$ = 9.6 Hz, 1H), 8.15 (dd, $^3J_{HH}$ = 9.6 Hz, $^3J_{HH}$ = 2.4 Hz, 1H), 7.97 (dd, $^3J_{HH}$ = 8.4 Hz, $^3J_{HH}$ = 6.0 Hz, 1H), 7.76 (d, $^3J_{HH}$ = 6.8 Hz, 2H), 7.69 (d, $^3J_{HH}$ = 6.8 Hz, 1H), 7.61 (s, 1H), 7.49 (t, $^3J_{HH}$ = 7.4 Hz, 1H), 7.41–7.36 (m, 4H), 6.11 (s, 2H). ^{13}C{^{1}H} NMR (100.6 MHz, 298 K, DMSO-d_6); δ 169.4, 148.8, 148.6, 140.1, 135.8, 135.6, 134.0, 133.7, 133.4, 133.2, 132.1, 130.9, 130.6, 129.9, 129.7, 128.5, 123.4, 120.6, 119.6, 62.0; ^{11}B NMR (160 MHz, 297 K, CD_3OD); δ 28.6; HRMS-ESI$^+$ (*m*/*z*): calculated for $[C_{23}H_{20}BN_2O_3]^+$ 383.15615, found 383.15663. ATR-IR ν (cm^{-1}): 3354br, 1667m, 1548s, 1357s, 1330s, 1257s, 705s and 637m.

Crystallographic investigations. The relevant details of crystal **11-SO$_4$**, data collection and structure refinement can be found in Table S1.† Data collection for sulfate salt of **11-SO$_4$** was performed at 273 K using M_oK_α radiation (0.71073 Å) on a Bruker APEX II CCD from an Incoatec ImuS source and Helios optic monochromator.[63] Suitable crystal was coated with hydrocarbon oil, picked up with a nylon loop, and mounted on the cold nitrogen stream of the diffractometer. The structures were solved by direct methods[64] and refined by full-matrix least-squares on F^2 using the shelXle GUI.[65,66]

The hydrogen atoms of the C–H bonds were placed in idealized positions whereas the hydrogen atoms from the N–H and O–H moieties were localized from the difference electron density map and their position was refined with U_{iso} tied to the parent atom with distance restraints (DFIX).

Compound **11-SO4** presents positional disorder in DMSO solvent in two positions whit a ratio 95/5. The model of two positions was refined using geometry (SAME) and U_{ij} restraints (SIMU, RIGU) implemented in SHELXL. The occupancy of two molecules of water was refined with free variables shown occupancy of 71% and 49% respectively. The molecular graphics were prepared using OLEX.[67] Crystallographic data for crystal structure has been deposited with the Cambridge Crystallographic Data Centre no 2281178.† X-ray crystallographic data in CIF format are available in ESI.†

Fluorimetric titrations. Titration experiments were performed by adding aliquots of stock solutions of diols to buffered aqueous solutions (10 mM MOPS at pH 7.4) of bromide salts of **11–13** (20 μM). After adding the concentrated solution of diols, the solution was stirred for 1.0 min. at r. t. to achieve equilibrium before recording the emission spectrum (λ_{ex} = 350 nm for **11-12**, λ_{ex} = 325 for **13** and 650 V for all cases) using a quartz cuvette. Lifetimes were measured according to the procedure reported in the ref. 60 Instrumental and experimental details are described in the ESI.†

NMR spectroscopy studies. ^{1}H-NMR titration experiment was carried out by adding increasing amounts of sorbitol (0–4.0 equiv.) to a solution of **11** (2 mM) in DMSO-d_6. After each sorbitol addition, the sample was sonicated for 1.0 min and spectra were recorded on a 300 MHz spectrometer at 298 K. ^{11}B NMR spectra of **11** (4.0 mM) with 12 equiv. of sorbitol were obtained in CD_3OD-D_2O at r. t. and subsequently at lower temperatures (233 K; 160.5 MHz) in a quartz NMR tube.

Conflicts of interest

There are no conflicts to declare.

Acknowledgements

This work was financially supported by grants: PAPIIT-UNAM-220023 and CONACYT PRONACES-160671. We thank M. Sc. Eréndira García Rios, M. Sc. Lucero Mayra Ríos Ruiz, M. Sc. Lucía del Carmen Márquez Alonso, M. Sc. Lizbeth Triana Cruz, M. Sc. Hortensia Segura Silva, Dra. Beatriz Quiroz-García, Dra. Adriana Romo Pérez, and M. Sc. Elizabeth Huerta Salazar for technical assistance. J. Z. M. is grateful to DGAPA-UNAM for a postdoctoral scholarship. M. K. S. F., J. V. G. and C. P. V. are grateful to CONAHCyT for scholarships 848759, 848787 and 812567 respectively. J. B. F. is grateful to DGTIC-UNAM for the use of the supercomputer Miztli.

References

1 G. T. Williams, J. L. Kedge and J. S. Fossey, Molecular Boronic Acid-Based Saccharide Sensors, *ACS Sens.*, 2021, **6**, 1508–1528.
2 X. Zhang, G. Liu, Z. Ning and G. Xing, Boronic acid-based chemical sensors for saccharides, *Carbohydr. Res.*, 2017, **452**, 129–148.
3 S. D. Bull, M. G. Davidson, J. M. H. V. A. N. D. E. N. Elsen, J. S. Fossey, A. T. a Jenkins, Y. Jiang, Y. Kubo, F. Marken, K. Sakurai, J. Zhao and T. D. James, Exploiting the Reversible Covalent Bonding of Boronic Acids: Recognition, Sensing, and Assembly, *Acc. Chem. Res.*, 2013, **46**, 312–326.
4 K. Lacina, P. Skládal and T. D. James, Boronic acids for sensing and other applications - a mini-review of papers published in 2013, *Chem. Cent. J.*, 2014, **8**, 1–17.
5 J. S. Fossey, F. D'Hooge, J. M. H. Van Den Elsen, M. P. Pereira Morais, S. I. Pascu, S. D. Bull, F. Marken, A. T. A. Jenkins, Y. B. Jiang and T. D. James, The development of boronic acids as sensors and separation tools, *Chem. Rec.*, 2012, **12**, 464–478.
6 X. Sun, W. Zhai, J. S. Fossey and T. D. James, Boronic acids for fluorescence imaging of carbohydrates, *Chem. Commun.*, 2016, **52**, 3456–3469.
7 S. L. Tong, Z. Y. Tian, Y. H. Wu, Y. Yan, S. Hu and J. Yu, Crystal assembly based on 3,5-bis(2′-benzimidazole) pyridine and its complexes, *Solid State Sci.*, 2013, **17**, 6–13.
8 J. S. Hansen, M. Ficker, J. F. Petersen, J. B. Christensen and T. Hoeg-Jensen, Ortho-Substituted fluorescent aryl monoboronic acid displays physiological binding of d-glucose, *Tetrahedron Lett.*, 2013, **54**, 1849–1852.
9 J. N. Cambre and B. S. Sumerlin, Biomedical applications of boronic acid polymers, *Polym.*, 2011, **52**, 4631–4643.
10 A. Stubelius, S. Lee and A. Almutairi, The Chemistry of Boronic Acids in Nanomaterials for Drug Delivery, *Acc. Chem. Res.*, 2019, **52**, 3108–3119.
11 Z. Bian, A. Liu, Y. Li, G. Fang, Q. Yao, G. Zhang and Z. Wu, Boronic acid sensors with double recognition sites: A review, *Analyst*, 2020, **145**, 719–744.
12 C. Chen, G. El Khoury, P. Zhang, P. M. Rudd and C. R. Lowe, *J. Chromatogr. A*, 2016, **1444**, 8–20.
13 M. D. Heagy and R. K. Meka, Fluorescent and Colorimetric Probes for Carbohydrates: A Second Decade's Worth of Bright Spies for Saccharides, in *Comprehensive Supramolecular Chemistry II*, ed. J. L. Atwood, Elsevier, Oxford, 2017, pp. 615–647.
14 W. Zhai, X. Sun, T. D. James and J. S. Fossey, Boronic Acid-Based Carbohydrate Sensing, *Chem. Asian J.*, 2015, **10**, 1836–1848.
15 S. Craig, Synthesis and evaluation of aryl boronic acids as fluorescent artificial receptors for biological carbohydrates, *Bioorg. Chem.*, 2012, **40**, 137–142.
16 R. Hosseinzadeh, M. Mohadjerani and M. Pooryousef, Fluorene-based boronic acids as fluorescent chemosensor for monosaccharides at physiological pH, *Luminescence*, 2015, **30**, 549–555.
17 C. Hoffmann, M. Jourdain, A. Grandjean, A. Titz and G. Jung, β-Boronic Acid-Substituted Bodipy Dyes for Fluorescence Anisotropy Analysis of Carbohydrate Binding, *Anal. Chem.*, 2022, **94**, 6112–6119.
18 C. R. Cooper and T. D. James, Selective D-glucosamine hydrochloride fluorescence signalling based on ammonium cation and diol recognition, *Chem. Commun.*, 1997, 1419–1420.
19 A. Chaicham, S. Sahasithiwat, T. Tuntulani and B. Tomapatanaget, Highly effective discrimination of catecholamine derivatives via FRET-on/off processes induced by the intermolecular assembly with two fluorescence sensors, *Chem. Commun.*, 2013, **49**, 9287–9289.
20 M. Debiais, J. J. Vasseur and M. Smietana, Applications of the Reversible Boronic Acids/Boronate Switch to Nucleic Acids, *Chem. Rec.*, 2022, **22**, 1–16.
21 A. E. Hargrove, R. N. Reyes, I. Riddington, E. V. Anslyn and J. L. Sessler, Boronic acid porphyrin receptor for ginsenoside sensing, *Org. Lett.*, 2010, **12**, 4804–4807.
22 P. M. Chaudhary, R. V. Murthy, R. Yadav and R. Kikkeri, A rationally designed peptidomimetic biosensor for sialic acid on cell surfaces, *Chem. Commun.*, 2015, **51**, 8112–8115.
23 K. S. Ahn, J. H. Lee, J. M. Park, H. N. Choi and W. Y. Lee, Luminol chemiluminescence biosensor for glycated hemoglobin (HbA1c) in human blood samples, *Biosens. Bioelectron.*, 2016, **75**, 82–87.
24 X. Huang, Y. Han, J. Li, M. Tang and G. Qing, Sensitive and specific detection of saccharide species based on fluorescence: update from 2016, *Anal. Bioanal. Chem.*, 2023, **415**, 4061–4077.
25 J. A. Peters, Interactions between boric acid derivatives and saccharides in aqueous media: Structures and stabilities of resulting esters, *Coord. Chem. Rev.*, 2014, **268**, 1–22.
26 G. F. Whyte, R. Vilar and R. Woscholski, Molecular recognition with boronic acids — applications in chemical biology, *J. Chem. Biol.*, 2013, **6**, 161–174.
27 J. Krämer, R. Kang, L. M. Grimm, L. De Cola, P. Picchetti and F. Biedermann, Molecular Probes, Chemosensors, and Nanosensors for Optical Detection of Biorelevant

Molecules and Ions in Aqueous Media and Biofluids, *Chem. Rev.*, 2022, **122**, 3459–3636.
28 W. L. A. Brooks, C. C. Deng and B. S. Sumerlin, Structure–Reactivity Relationships in Boronic Acid–Diol Complexation, *ACS Omega*, 2018, **3**, 17863–17870.
29 J. Yan, G. Springsteen, S. Deeter and B. Wang, The relationship among pKa, pH, and binding constants in the interactions between boronic acids and diols—it is not as simple as it appears, *Tetrahedron*, 2004, **60**, 11205–11209.
30 G. Springsteen and B. Wang, A detailed examination of boronic acid-diol complexation, *Tetrahedron*, 2002, **58**, 5291–5300.
31 S. Harnsoongnoen and A. Wanthong, Real-time monitoring of sucrose, sorbitol, D-glucose and D-fructose concentration by electromagnetic sensing, *Food Chem.*, 2017, **232**, 566–570.
32 G. Fang, Z. Bian, D. Liu, G. Wu, H. Wang, Z. Wu and Q. Yao, Water-soluble diboronic acid-based fluorescent sensors recognizing d-sorbitol, *New J. Chem.*, 2019, **43**, 13802–13809.
33 M. S. Badiga, N. K. Jain, C. Casanova and C. S. Pitchumoni, Diarrhea in diabetics: the role of sorbitol, *J. Am. Coll. Nutr.*, 1990, **9**, 578–582.
34 X. Wu, X.-X. Chen and Y. B. Jiang, Recent advances in boronic acid-based optical chemosensors, *Analyst*, 2017, **142**, 1403–1414.
35 K. Sugita, Y. Suzuki, Y. Tsuchido, S. Fujiwara, T. Hashimoto and T. Hayashita, A simple supramolecular complex of boronic acid-appended β-cyclodextrin and a fluorescent boronic acid-based probe with excellent selectivity for d-glucose in water, *RSC Adv.*, 2022, **12**, 20259–20263.
36 Y. Suzuki, Y. Mizuta, A. Mikagi, T. Misawa-Suzuki, Y. Tsuchido, T. Sugaya, T. Hashimoto, K. Ema and T. Hayashita, Recognition of d -Glucose in Water with Excellent Sensitivity, Selectivity, and Chiral Selectivity Using γ-Cyclodextrin and Fluorescent Boronic Acid Inclusion Complexes Having a Pseudo-diboronic Acid Moiety, *ACS Sens.*, 2023, **8**, 218–227.
37 A. Schiller, R. A. Wessling and B. Singaram, A fluorescent sensor array for saccharides based on boronic acid appended bipyridinium salts, *Angew. Chem., Int. Ed.*, 2007, **46**, 6457–6459.
38 T. D. James, H. Shinmori and S. Shinkai, Novel fluorescence sensor for "small" saccharides, *Chem. Commun.*, 1997, 71–72.
39 K. M. K. Swamy, Y. J. Jang, M. S. Park, H. S. Koh, S. K. Lee, Y. J. Yoon and J. Yoon, A sorbitol-selective fluorescence sensor, *Tetrahedron Lett.*, 2005, **46**, 3453–3456.
40 X. Liang, T. D. James and J. Zhao, 6,6′-Bis-substituted BINOL boronic acids as enantioselective and chemoselective fluorescent chemosensors for d-sorbitol, *Tetrahedron*, 2008, **64**, 1309–1315.
41 H. Wang, G. Fang, H. Wang, J. Dou, Z. Bian, Y. Li, H. Chai, Z. Wu and Q. Yao, A diboronic acid fluorescent sensor for selective recognition of d-ribose via fluorescence quenching, *New J. Chem.*, 2019, **43**, 4385–4390.
42 S. Liu, H. Bai, Q. Sun, W. Zhang and J. Qian, Naphthalimide-based fluorescent photoinduced electron transfer sensors for saccharides, *RSC Adv.*, 2015, **5**, 2837–2843.
43 S. Akay, W. Yang, J. Wang, L. Lin and B. Wang, Synthesis and evaluation of dual wavelength fluorescent benzo[b] thiophene boronic acid derivatives for sugar sensing, *Chem. Biol. Drug Des.*, 2007, **70**, 279–289.
44 R. Badugu, J. R. Lakowicz and C. D. Geddes, Fluorescence sensors for monosaccharides based on the 6-methylquinolinium nucleus and boronic acid moiety: Potential application to ophthalmic diagnostics, *Talanta*, 2005, **65**, 762–768.
45 R. Badugu, J. R. Lakowicz and C. D. Geddes, Boronic acid fluorescent sensors for monosaccharide signaling based on the 6-methoxyquinolinium heterocyclic nucleus: Progress toward noninvasive and continuous glucose monitoring, *Bioorg. Med. Chem.*, 2005, **13**, 113–119.
46 R. Badugu, J. R. Lakowicz and C. D. Geddes, A wavelength-ratiometric fluoride-sensitive probe based on the quinolinium nucleus and boronic acid moiety, *Sens. Actuators, B*, 2005, **104**, 103–110.
47 J. Valdes-García, J. Zamora-Moreno, M. K. Salomón-Flores, D. Martínez-Otero, J. Barroso-Flores, A. K. Yatsimirsky, I. J. Bazany-Rodríguez and A. Dorazco-González, Fluorescence Sensing of Monosaccharides by Bis-boronic Acids Derived from Quinolinium Dicarboxamides: Structural and Spectroscopic Studies, *J. Org. Chem.*, 2023, **88**, 2174–2189.
48 I. J. Bazany-Rodríguez, M. K. Salomón-Flores, A. O. Viviano-Posadas, M. A. García-Eleno, J. Barroso-Flores, D. Martínez-Otero and A. Dorazco-González, Chemosensing of neurotransmitters with selectivity and naked eye detection ofl-DOPA based on fluorescent Zn(ii)-terpyridine bearing boronic acid complexes, *Dalton Trans.*, 2021, **50**, 4255–4269.
49 A. O. Viviano-Posadas, U. Romero-Mendoza, I. J. Bazany-Rodríguez, R. V. Velázquez-Castillo, D. Martínez-Otero, J. M. Bautista-Renedo, N. González-Rivas, R. Galindo-Murillo, M. K. Salomón-Flores and A. Dorazco-González, Efficient fluorescent recognition of ATP/GTP by a water-soluble bisquinolinium pyridine-2,6-dicarboxamide compound. Crystal structures, spectroscopic studies and interaction mode with DNA, *RSC Adv.*, 2022, **12**, 27826–27838.
50 S. O. Kang, T. S. Johnson, V. W. Day and K. Bowman-James, Pyridine-2,6-dicarboxamide pincer-based macrocycle: a versatile ligand for oxoanions, oxometallates, and transition metals, *Supramol. Chem.*, 2018, **30**, 305–314.
51 P. Kumar and R. Gupta, The wonderful world of pyridine-2,6-dicarboxamide based scaffolds, *Dalton Trans.*, 2016, **45**, 18769–18783.
52 A. Dorazco-González, H. Höpfl, F. Medrano and A. K. Yatsimirsky, Recognition of anions and neutral guests by dicationic pyridine-2,6-dicarboxamide receptors, *J. Org. Chem.*, 2010, **75**, 2259–2273.
53 I. J. Bazany-Rodríguez, D. Martínez-Otero, J. Barroso-Flores, A. K. Yatsimirsky and A. Dorazco-González, Sensitive water-soluble fluorescent chemosensor for chloride based on a bisquinolinium pyridine-dicarboxamide compound, *Sens. Actuators, B*, 2015, **221**, 1348–1355.

54 W. F. Jager, T. S. Hammink, O. van den Berg and F. C. Grozema, Highly sensitive water-soluble fluorescent ph sensors based on the 7-amino-1-methylquinolinium chromophore, *J. Org. Chem.*, 2010, **75**, 2169–2178.

55 K. Tanabe, Y. Suzui, M. Hasegawa and T. Kato, Full-color tunable photoluminescent ionic liquid crystals based on tripodal pyridinium, pyrimidinium, and quinolinium salts, *J. Am. Chem. Soc.*, 2012, **134**, 5652–5661.

56 A. Dorazco-González, M. F. Alamo, C. Godoy-Alcántar, H. Höpfl and A. K. Yatsimirsky, Fluorescent anion sensing by bisquinolinium pyridine-2,6-dicarboxamide receptors in water, *RSC Adv.*, 2014, **4**, 455.

57 P. Thordarson, Determining association constants from titration experiments in supramolecular chemistry, *Chem. Soc. Rev.*, 2011, **40**, 1305–1323.

58 B. M. Chapin, P. Metola, S. L. Vankayala, H. L. Woodcock, T. J. Mooibroek, V. M. Lynch, J. D. Larkin and E. V. Anslyn, Disaggregation is a Mechanism for Emission Turn-On of ortho-Aminomethylphenylboronic Acid-Based Saccharide Sensors, *J. Am. Chem. Soc.*, 2017, **139**, 5568–5578.

59 X. Wu, Z. Li, X.-X. Chen, J. S. Fossey, T. D. James and Y.-B. B. Jiang, Selective sensing of saccharides using simple boronic acids and their aggregates, *Chem. Soc. Rev.*, 2013, **42**, 8032–8048.

60 M. K. Salomón-Flores, C. L. Hernández-Juárez, I. J. Bazany-Rodríguez, J. Barroso-Flores, D. Martínez-Otero, R. López-Arteaga, J. Valdés-Martínez and A. Dorazco-González, Efficient fluorescent chemosensing of iodide based on a cationic meso-tetraarylporphyrin in pure water, *Sens. Actuators, B*, 2019, **281**, 462–470.

61 S. Gamsey, N. A. Baxter, Z. Sharrett, D. B. Cordes, M. M. Olmstead, R. A. Wessling and B. Singaram, The effect of boronic acid-positioning in an optical glucose-sensing ensemble, *Tetrahedron*, 2006, **62**, 6321–6331.

62 S. Arimori, M. L. Bell, C. S. Oh and T. D. James, A modular fluorescence intramolecular energy transfer saccharide sensor, *Org. Lett.*, 2002, **4**, 4249–4251.

63 APEX 2 Software Suite, *APEX 2 Software Suite*, Bruker AXS Inc., Madison, Wisconsin, USA.

64 G. M. Sheldrick, SHELXT - Integrated space-group and crystal-structure determination, *Acta Crystallogr. A*, 2015, **71**, 3–8.

65 C. B. Hübschle, G. M. Sheldrick and B. Dittrich, ShelXle: A Qt graphical user interface for SHELXL, *J. Appl. Crystallogr.*, 2011, **44**, 1281–1284.

66 G. M. Sheldrick, *SHELXL-97, Progr. Cryst. Struct. Refinement*, Univ. Göttingen.

67 O. V. Dolomanov, L. J. Bourhis, R. J. Gildea, J. A. K. Howard and H. Puschmann, OLEX2: A complete structure solution, refinement and analysis program, *J. Appl. Crystallogr.*, 2009, **42**, 339–341.